Controlled dielectrophoretic assembly of carbon nanotubes using real-time electrical detection

Sebastian Sorgenfrei,[1,a)] Inanc Meric,[1] Sarbajit Banerjee,[2] Austin Akey,[3] Sami Rosenblatt,[1] Irving P. Herman,[3] and Kenneth L. Shepard[1]
[1]*Department of Electrical Engineering, Columbia University, New York, New York 10027, USA*
[2]*Department of Chemistry, University of Buffalo, Buffalo, New York 14260-3000, USA*
[3]*Department of Applied Physics and Applied Mathematics, Columbia University, New York, New York 10027, USA*

(Received 13 July 2008; accepted 5 January 2009; published online 2 February 2009)

We investigate dielectrophoretic deposition of single-walled carbon nanotubes using an *in situ* detection system. Pairs of electrodes are stimulated with a small-amplitude, low-frequency voltage superimposed on a large-amplitude, high-frequency dielectrophoretic voltage. Measuring the magnitude of the current both at dc (I_{dc}) and at the low frequency (I_{ac}) through a digital lock-in technique allows us to determine when a nanotube has made electrical contact and to halt the dielectrophoretic process. Because I_{dc} is determined by nonlinearities in the device current-voltage characteristic, measurement of the I_{dc}/I_{ac} ratio allows the real-time determination of whether the deposited nanotube is metallic or semiconducting. © *2009 American Institute of Physics*.
[DOI: 10.1063/1.3077620]

Single-walled carbon nanotubes (SWCNTs) have shown great promise for application in future electronic devices because of their very high mobilities and inherently nanoscale geometry.[1] SWCNTs have been used to fabricate field effect transistors[2] and photovoltaic devices,[3] as well as chemical[4] and biological sensors[5] based on field-effect structures. These applications all require controlled assembly of nanotubes, which is accomplished with controlled growth and technologies to transfer tubes after growth to a desired substrate. Because high growth temperatures are incompatible with traditional semiconductor processes, transfer techniques have been pursued including spin coating of nanotubes from suspensions[6] and mechanical transfer,[7] but these approaches do not provide substantial control over the precise positioning and alignment of nanotubes within device structures. As an alternative, radio frequency dielectrophoresis (DEP) can be used to align polarizable nanotubes through gradients in an applied electric field.[8] The dielectrophoretic force on a ballistic nanotube can be expressed as[9]

$$\bar{F}_{\mathrm{DEP}} \propto \varepsilon_m \frac{\varepsilon_p - \varepsilon_m}{\varepsilon_p + 2\varepsilon_m} \nabla E^2, \qquad (1)$$

where ε_p and ε_m are the dielectric constants of the particle and the medium and E is the magnitude of the electric field.

A recent report demonstrates real-time detection of dielectrophoretically trapped multiwalled carbon nanotubes by measuring a decrease in the gap impedance.[10] To the best of our knowledge there have been no reports of the *in situ* control of the dielectrophoretic assembly of SWCNTs, which represents a significantly more formidable challenge because of the much smaller dimensions involved, the variability in chirality, and the concomitant complexity in the measured electrical response. Our approach not only enables the real-time determination of the trapping of a carbon nanotube, but also allows evaluation of the metallic/semiconducting nature of the trapped species.

The lock-in detection system is shown in Fig. 1(a) and is implemented on a custom printed circuit board. Two ac potentials are superimposed through a summing amplifier: a signal at $f_2 = 5$ MHz, which is used to manipulate the carbon nanotubes, and a signal at $f_1 = 1$ kHz, with constant 100 mV amplitude.[11] Both the dc (I_{dc}) and the f_1-component (I_{ac}) of the device conductance are monitored in real time. Microelectrodes were made by standard electron-beam lithography (5/50 nm Cr/Au) on a glass substrate in order to limit the fringing fields from the electrodes to the substrate, reducing the number of tubes attaching to the sides of the electrodes away from the gap. Since nanotube lengths range from 500 nm to 3 μm, a gap of 1 μm was chosen so that most deposited nanotubes can bridge the gap.

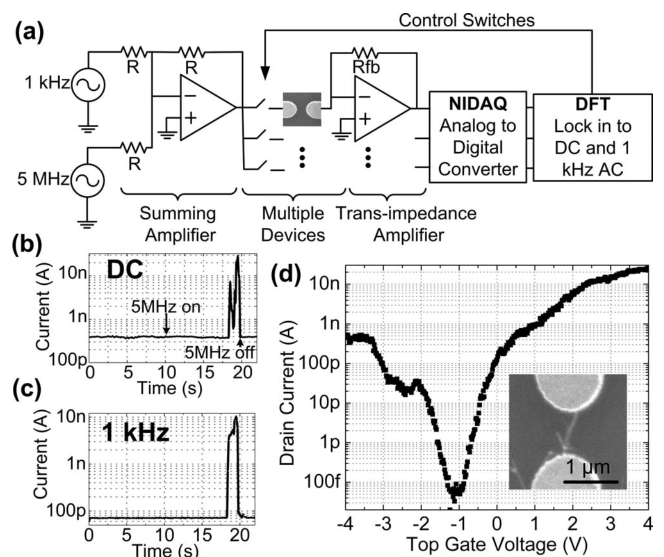

FIG. 1. (a) Lock-in detection setup allowing DEP to proceed along with real-time measurement. [(b) and (c)] Real-time measurements during DEP deposition of I_{dc} and I_{ac}, respectively. (d) I_{ds} as a function of V_{gs} for V_{ds} = 100 mV of top-gated device fabricated from deposited nanotube. Inset shows SEM of the deposited nanotube.

[a)]Electronic mail: sfs2102@columbia.edu.

 © 2009 American Institute of Physics

Author complimentary copy. Redistribution subject to AIP license or copyright, see http://apl.aip.org/apl/copyright.jsp

The carbon nanotubes used in this experiment were synthesized by the arc discharge method (from Carbon Solutions) and dispersed in 1,2 dichloroethane (DCE) by ultrasonication for 2 h and centrifugation at 8000 rpm for 2 h, resulting in a concentration of approximately 6 ng/ml. DCE (with $\varepsilon_m \cong 10.3$) has been used extensively in the past to disperse SWCNTs,[12] and the quality of the resulting suspension used for this experiment was verified through ultraviolet-visible spectroscopy, which compares to published data for suspensions containing both metallic and semiconducting nanotubes.[13] DCE suspension allows surfactants to be avoided, which coats nanotubes and affects contact resistance. Several other solvents were tried to disperse nanotubes, including acetone, isopropanol, ethanol, toluene, and methanol, but did not result in stable suspensions.

From Eq. (1), metallic SWCNTs have a very large dielectric constant ($\varepsilon_p \gg \varepsilon_m$) such that the dielectrophoretic force is positive for any diameter ($\bar{F}_{\mathrm{DEP}} \propto \varepsilon_m \nabla E_{\mathrm{rms}}^2$). Semiconducting nanotubes, however, have a dielectric constant that varies with their bandgap as $\varepsilon_p \cong 1+(\hbar\omega_p/5.4E_g)^2$.[8] Assuming $E_g=|t|a_{cc}/d$ with the energy of the plasma frequency $\hbar\omega_p \approx 5$ eV, the graphite overlap integral $|t|=2.5$ eV and the nearest neighbor distance $a_{cc}=0.142$ nm, $\bar{F}_{\mathrm{DEP}}$ as a function of tube diameter has the relation shown in Fig. 3(b). Therefore for semiconducting nanotube with diameters smaller (larger) than 1.2 nm, the dielectrophoretic force is negative (positive).

A very simple protocol is used for DEP. A small drop of the suspension (40 μL) is introduced onto the chip at the area of the electrodes. The 2.5 V 5 MHz signal is turned off less than 2 s after a change in both I_{ac} and I_{dc} is observed, avoiding the deposition of multiple tubes across the gap. After deposition, the chip is carefully rinsed with DCE and isopropanol followed by a gentle dry in nitrogen. This light rinsing is necessary because, otherwise, the nanotube suspension will dry and nanotubes will be dispersed randomly on the surface. We have never seen a case when a bridged tube was removed through rinsing. The devices are imaged with a scanning electron microscope (SEM) and atomic force microscopy (AFM) to determine how many nanotubes bridge each electrode pair. The electrical properties of the deposited nanotubes are independently characterized by creating a top gate by depositing 15 nm of hafnium oxide by atomic layer deposition and a gate electrode through electron-beam lithography.

The results from a representative DEP deposition are shown in Figs. 1(b)–1(d). Figures 1(b) and 1(c) show I_{ac} and I_{dc} as a function of time; deposition stops at $t=20$ s. A clear change in the current magnitudes is evident at $t=18$ s as the electrodes are connected by a deposited nanotube. The SEM image of the inset in Fig. 1(d) confirms that a single tube (or small bundle) connects the electrodes. Figure 1(d) shows the subthreshold characteristics of the deposited nanotube device at $V_{\mathrm{ds}}=0.1$ V, demonstrating an $I_{\mathrm{on}}/I_{\mathrm{off}}$ ratio of 10^5 and a subthreshold slope of 240 mV/decade. Contact resistances generally range from 500 kΩ–10 MΩ, consistent with other reported results for gold bottom contacts.[14]

In order to understand the increase in I_{ac} and I_{dc} when a nanotube bridges the electrodes, the nanotube device is modeled as a Schottky barrier with a series resistance, so that the current-voltage characteristics of the nanotube can be approximated by[3,15]

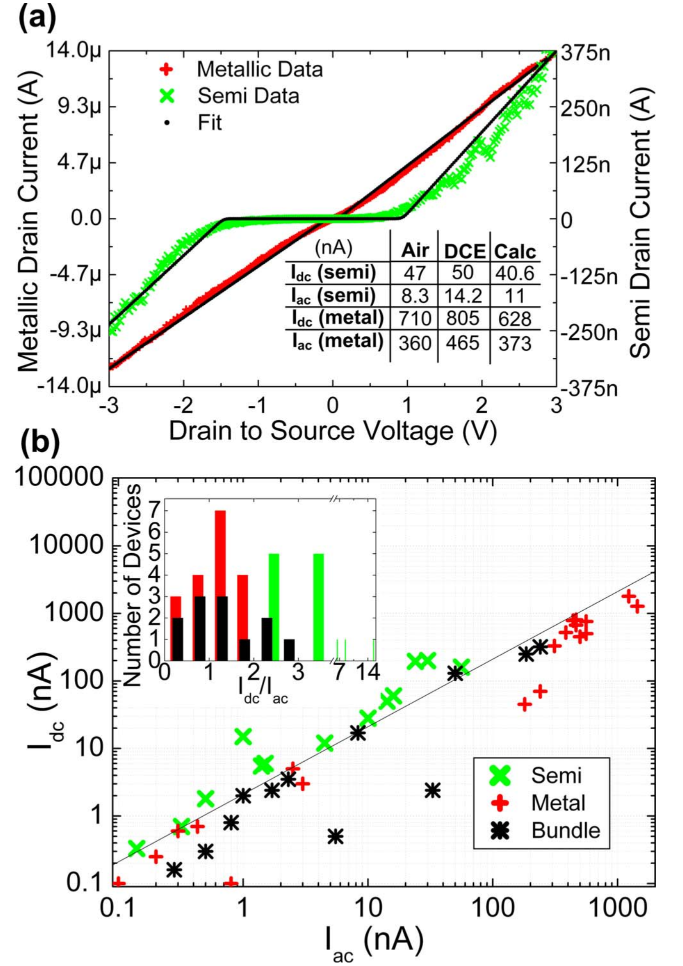

FIG. 2. (Color online) (a) Drain current (I_{ds}) as a function of drain to source voltage (V_{ds}) for a typical semiconducting and a metallic carbon nanotube. Measured data and the associated fit to Eq. (2) are shown. (b) Distribution of I_{ac} and I_{dc} values for 43 representative nanotube devices. Inset shows histogram binning of the $I_{\mathrm{dc}}/I_{\mathrm{ac}}$ ratio.

$$I=\frac{k_BT}{qR_D}\ln\left\{1+\frac{I_{0D}qR_D}{k_BT}e^{[(q/k_BT)V+(I_{0D}qR_D/k_BT)]}\right\}-I_{0D}-\frac{k_BT}{qR_S}\ln\left\{1+\frac{I_{0S}qR_S}{k_BT}e^{[-(q/k_BT)V+(I_{0S}qR_S/k_BT)]}\right\}+I_{0S}, \quad (2)$$

where R_D and R_S are the resistance of drain and source, I_{0D} and I_{0S} are the diode drain and source saturation currents, q is the electric charge, V is the applied drain-to-source bias, T is the temperature, and k_B is Boltzmann's constant. In Fig. 2(a), this equation is fit to a high bias drain to source sweep of a representative semiconductor and a representative metallic nanotube with I_{0D}, I_{0S}, R_D, and R_S as fitting parameters. Because the saturation currents I_{0D} and I_{0S} increase exponentially with decreasing barrier height, one finds that for metallic nanotubes, $I_{0D} \gg kT/qR_D$ and $I_{0S} \gg kT/qR_S$. In this case, a nearly linear relation results with $I \cong V/R_D$ for $V>0$ and $I \cong V/R_S$ for $V<0$. In contrast, semiconducting nanotubes have large, unequal source and drain barriers, resulting in very nonlinear and asymmetric current-voltage characteristics. We can use Eq. (2) and a Fourier analysis to estimate the I_{dc} and I_{ac} values that result from the applied potential $V=A_{1\ \mathrm{kHz}}\cos(2\pi f_1 t)+A_{5\ \mathrm{MHz}}\cos(2\pi f_2 t)$. The table in Fig. 2(a) shows the calculated values that result for the two characterized tubes. These match closely those measured in air

Author complimentary copy. Redistribution subject to AIP license or copyright, see http://apl.aip.org/apl/copyright.jsp

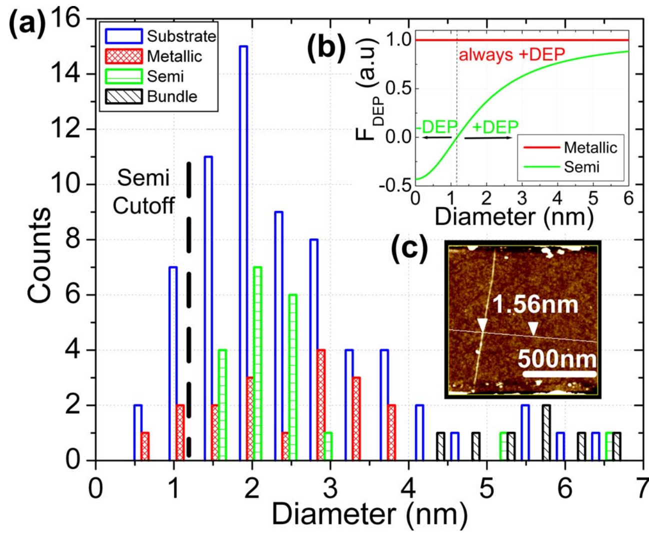

FIG. 3. (Color online) (a) Diameter distribution for nanotubes randomly dispersed on substrate and metallic, semiconducting and bundled nanotubes deposited by DEP. (b) Clausius Mossotti function for metallic and semiconducting nanotubes. (c) A representative AFM image of single tube.

and in DCE before creating the top gate. Large I_{ac} values are observed when the electrodes are bridged in Fig. 1(c) due to the fact that the large-amplitude 5 MHz signal moves the bias point throughout the whole curve to increase the conductance at f_1, even for semiconducting devices that do not have significant conduction for small applied biases.

In Fig. 2(b), the results for 43 representative devices are plotted as a function of I_{dc} and I_{ac}. Semiconducting nanotubes are characterized by I_{on}/I_{off} ratios greater than 3 and $I_{off} < 10$ pA as measured for top-gated field-effect structures fabricated from these nanotubes, while metallic nanotubes are characterized by I_{on}/I_{off} ratio of 3 or smaller. Devices with I_{on}/I_{off} ratios in excess of 3 but without a bandgap ($I_{off} > 10$ pA) are called bundles. The inset of Fig. 2(b) indicates how the I_{dc}/I_{ac} ratio can be used to distinguish metallic from semiconducting tubes during DEP. I_{dc}/I_{ac} ratios of greater than 2 are a confident indicator of semiconducting tubes, while I_{dc}/I_{ac} ratios of less than 2 are a confident indicator of metallic tubes or bundles.

Figure 3(a) shows the distribution of tubes randomly dispersed on a substrate (labeled "substrate") and the distributions of metallic, semiconducting, and bundled nanotubes, as characterized by their electronic properties, which are deposited by DEP. We only count devices with a single bridging nanotube as verified by AFM [Fig. 3(c)]. The distributions for single nanotubes are centered around 1.6–2.1 nm indicating that nanotubes are being deposited in a manner that closely matches the original distribution of the nanotube soot.[13] It is important to note that semiconducting nanotubes with diameters less than 1.2 nm are not present, consistent with the prediction of Fig. 3(b). As a result, there is a slightly higher affinity for metallic tubes, resulting in deposition of metallic to semiconducting tubes in the ratio of 1:1 compared to 1:2 in the original distribution according to the specifications given by the supplier.

We presented a detection system to improve the controllability of carbon nanotube assembly through DEP. The demonstrated approach not only allows the real-time evaluation of the assembly process but also provides the ability to distinguish metallic from semiconducting tubes, paving the way for the precise placement of metallic or semiconducting nanotubes at specific sites within device architectures.

This work was supported in part by the NSF Nanoscale Science and Engineering Center at Columbia University, the New York State of Science, Technology, and Academic Research (NYSTAR), and the NSF under Contract No. 0707748.

[1]P. Avouris, Chem. Phys. **281**, 429 (2002).
[2]A. Javey, J. Guo, D. B. Farmer, Q. Wang, D. Wang, R. G. Gordon, M. Lundstrom, and H. Dai, Nano Lett. **4**, 447 (2004).
[3]J. U. Lee, Appl. Phys. Lett. **87**, 073101 (2005).
[4]J. Kong, N. R. Franklin, C. Zhou, M. G. Chapline, S. Peng, K. Cho, and H. Dai, Science **287**, 622 (2000).
[5]R. J. Chen, S. Bangsaruntip, K. A. Drouvalaksi, W. S. K. Nadine, M. Shim, Y. Li, W. Kim, P. J. Utz, and H. Dai, Proc. Natl. Acad. Sci. U.S.A. **100**, 4984 (2003).
[6]R. Martel, T. Schmid, H.R. Shea, T. Hertel, and P. Avouris, Appl. Phys. Lett. **73**, 2447 (1998).
[7]S.-H. Hur, O. O. Park, and J. A. Rogers, Appl. Phys. Lett. **86**, 243502 (2005).
[8]R. Krupke, F. Hennrich, H. B. Weber, M. M. Kappes, and H. v. Löhneysen, Nano Lett. **3**, 1019 (2003).
[9]R. Krupke, F. Hennrich, H. v. Löhneysen, and M. M. Kappes, Science **301**, 344 (2003).
[10]L. An and C. R. Friedrich, Appl. Phys. Lett. **92**, 173103 (2008).
[11]J. D. Beck, L. Shang, M. S. Marcus, and R. J. Hamers, Nano Lett. **5**, 777 (2005).
[12]S. J. Wind, J. Appenzeller, R. Martel, V. Derycke, and Ph. Avouris, Appl. Phys. Lett. **80**, 3817 (2002).
[13]M. E. Itkis, D. E. Perea, S. Niyogi, S. M. Rickard, M. A. Hamon, H. Hu, B. Zhao, and R. C. Haddon, Nano Lett. **3**, 309 (2003).
[14]R. Martel, T. Schmidt, H. R. Shea, T. Hertel, and Ph. Avouris, Appl. Phys. Lett. **73**, 2447 (1998).
[15]D. A. Barry, J.-Y. Parlange, L. Li, H. Prommer, C. J. Cunningham, and F. Stagnitti, Math. Comput. Simul. **53**, 95 (2000).

Author complimentary copy. Redistribution subject to AIP license or copyright, see http://apl.aip.org/apl/copyright.jsp